Branko RADIČEVIĆ[1], Milan SAVIĆ[2], Ion BADEA[3],
Žarko MILKIĆ[4], Peter RESPONDEK[5]

THE INFLUENCE OF WIND TURBINE BLADE ROTATION ON THE LIGHTNING STRIKE INCIDENCE

Abstract: The impact of wind turbine blade rotation on the lightning behavior is not sufficiently studied. The experimental results which are presented in this paper should enable a better understanding of this phenomenon. The tests were conducted in the high-voltage laboratory, applying the up-and-down method for determination of the 50% flash-over standard switching voltage. The impulse voltage waves were applied between the specially designed arching electrode and the blades of a reduced-size wind turbine model, driven by a frequency controlled motor. A lightning protection system in the form of receptors on the tips of the blades was examined. According to the theory of similarity the paper discusses the characteristics of direct atmospheric discharges for the several typical rotational speeds of the wind turbine. It was concluded that the number of direct lightning strikes in the zone of the air termination system on the blades is decreasing due to the rotation of the blades.

Key words: *air-termination system, arching electrode, blades, flashover voltage (FOV), induction motor, lightning protection, reduced-size model, rotation, up-and-down method, wind turbine*

1. INTRODUCTION

The development of power electronics and control systems, using double-fed induction generator and the synchronous generator with permanent magnets, the utilization of composite materials in the area of aeromechanics, and the increasing

[1] Mr Branko Radičević, asistent, Elektrotehnički fakultet, Bulevar kralja Aleksandra 73, 11120 Beograd, Srbija

[2] Prof. dr Milan Savić, Elektrotehnički fakultet, Bulevar kralja Aleksandra 73, 11120 Beograd, Srbija

[3] Eng. Ion Badea, ICMET – Research, Development, and Testing National Institute for Electrical Engineering, B-dul Decebal No.118A, 200746 Craiova, Romania

[4] Dr Žarko Milkić, Fakultet tehničkih nauka, Kneza Miloša 7, 38220 Kosovska Mitrovica, Srbija

[5] Eng. Peter Respondek, DEHN + SÖHNE GmbH + Co.KG., Hans-Dehn-Str. 1, D–92318 Neumarkt, Deutschland

need for the use of environmentally friendly energy sources have resulted in the incredible growth rate of installed wind turbines in the world and have enabled increase in physical dimensions and rated power of wind turbines.

The efficient protection of wind turbines against lightning is a very important because of their many specificities. Wind turbines are nonstandard structures with rotating elements being often placed at locations with poor grounding conditions and electrically interconnected in large wind farms are more vulnerable to lightning strikes [1], [2].

Current lightning air-termination systems for rotor blades are designed to withstand about 98% of lightning strikes, but there is still a risk of local damage, particularly at the attachment point [3], [4]. This percentage largely depends on the type of composite material used for manufacturing the rotor blades [nonconductive glass fibre reinforced polymers (GFRP) or semi-conductive carbon fibre composites (CFC)], the applied type of lightning protection system (LPS) for blades, and its length.

Almost all direct strikes to a wind turbine will hit the rotor blades which are the most expensive single component of the turbine and/or the windvane. More than 88% of lightning attachments occur within the outermost 1 m of the blade tip [5], but increased risk of inboard puncture for lightning strike of smaller current than 20 kA is also noticed [6].

The rotational speed of the blades w vary due to the stochastic nature of wind and for large wind turbines is between 0 and 25 r/min. A control system [7] provides the maximum possible electric power p_{el} at any moment and for each wind speed v_{wind}. Comparing the number of strikes to stationary wind turbines with the number of strikes to rotating blades in the same wind farm, during a very long period of time, is a possible approach to determine the impact of the wind turbine blade rotation on the incidence of lightning strikes. However, it is very difficult to implement in practice. For this reason the authors decided to build a reduced-size wind turbine model that was used to determine the influence of blade rotation on the lightning behavior.

2. EXPERIMENTAL RESEARCH

A reduced-size wind turbine model used in the impulse voltage tests is a modified version of commercial small wind turbine and also is a 1:40 scale model of an actual 3 MW wind turbine. A detailed model of the structure with arching electrode above the wind turbine in the high-voltage laboratory is shematically shown in Fig. 1.

The wind turbine model consists of the following main parts:

1) A three-bladed rotor is made of a composite insulating material (nonconductive glass fibre reinforced plastic). A knob-type copper receptors 2.5 cm in diameter were screwed into the both surfaces of each blade, 5 cm from the blade tip – Fig. 2(A). Receptors are manufactured from a copper alloy having excellent electrical and thermal qualities. Each receptor was bonded to the main laboratory grounding system by means of solid round copper down-conductor 10 mm in diameter inside of each blade. Therefore, when discharge hits the receptor on one of the blades, a surge current propagates through a down-conductor over the blade, a specially designed main shaft ball bearings (Fig. 2(C)) and the grounding conductor inside a tower to the main grounding system.

2) The main tower is an iron cylinder with a height of 3 m. The nacelle is also the iron cylinder without electric generator. Three-phase induction motor is placed into Faraday cage attached to the main tower near its top, with the purpose to run the wind turbine rotor by means of belt coupling (Fig. 2(D)). The rotational speed of the blades may be continually regulated in a range between 0–1000 rpm by a frequency converter. The standard surge protection with the commercially available surge arresters was installed to protect induction motor and frequency converter.

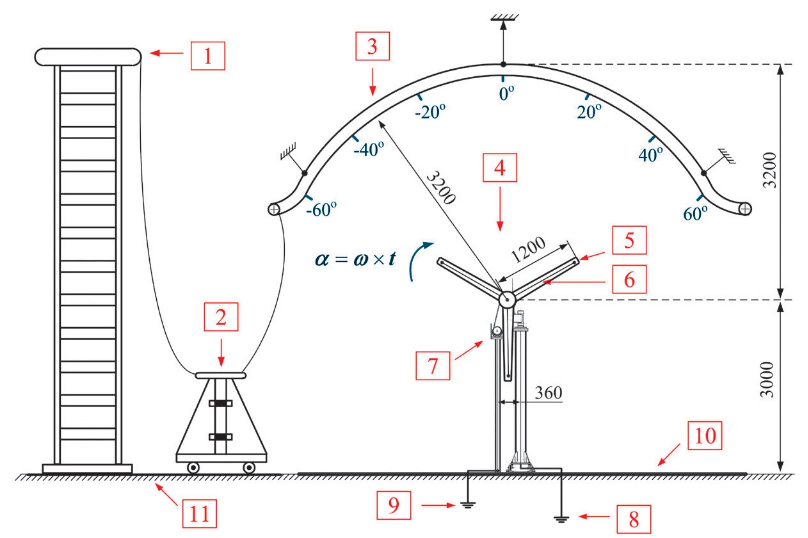

Front view: 1. Impulse generator; 2. Capacitive voltage divider; 3. High-voltage arching electrode; 4. 3-bladed wind turbine model; 5. Conductive receptor; 6. Down-conductor system; 7. Frequency-controlled induction motor; 8. Main grounding system of 4 Ω; 9. Auxiliary grounding system of 5.3 Ω; 10. Ground plane; 11. Laboratory floor. Note: All linear dimensions are in millimeters.

Figure 1. Experimental setup for reduced-size wind turbine model testing

3) Massive cross-like base with vibration absorbers, where the main and auxiliary wind turbine tower are bolted (Fig. 2(E)).

The authors also decided to build a special arching electrode to initiate the discharge development toward the wind turbine blade independent on the blade position, see Figs. 1 and 2(B). The arching electrode was constructed to provide constant distance from the electrode to the blade tips while the blades are rotating. The electrode was made from thin aluminum cylinder 15 cm in diameter reinforced by the arc-shaped steel tube whose length is 10 m and was fastened by several insulating ropes to prevent its movements. The blades and the arching electrode are in the same plane.

The optimal distance between the arching electrode and the top of the blades was set at 2 m for impulse voltages of negative polarity. According to the theory of similarity the scaling is very difficult, as well as the assessment how long sparks in the lab needs to be to represent actual lightning environment. It is also necessary to scale the velocity of the blade tip and the velocity of the streamers. Considering naturally occurring downward initiated lightning, the distance of 2 m corresponds to a minimum striking distance of 80 m, whereas the arching electrode represents the top of stepped leader before the last jump. During the testing, the streamers could easily be developed from the wind turbine model.

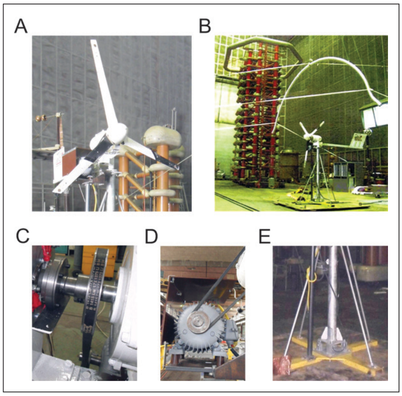

Figure 2. (A) Three-bladed wind turbine rotor with the conductive receptors at the blade tips; (B) Arching electrode set above the wind turbine model; (C) Main shaft ball bearings; (D) 4 kW frequency-controlled induction motor with belt coupling; (E) Cross-like base

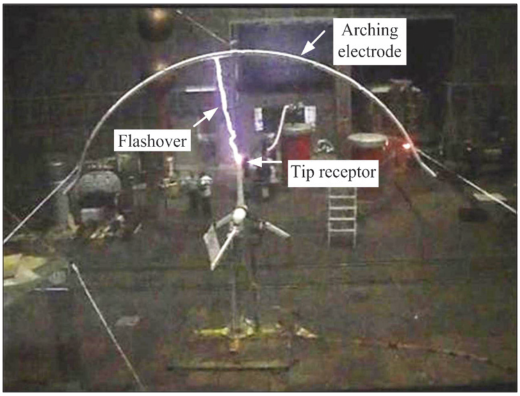

Figure 3. Photo from the control room when a negative impulse voltage is applied to the arching electrode

Based on the measured values at several characteristic points above the blades, it was concluded that the electric field is nearly uniform in the range $-45^{o} \leq \alpha \leq 45^{o}$ (Fig. 1). The field intensity about the blade tip is lowest when one of the blades is straight up ($\alpha = 0^{\circ}$) and slightly higher when one of the blades is straight down ($\alpha = 180^{\circ}$) due to somewhat higher charge density at the ends of the arching electrode. The arching electrode can provide a quasi-uniform field above the blade, less conducive to originating a discharge from it to approach the blade, or to represent a leader approaching from above the turbine, but mostly at its ends.

In order to minimize these effects the arching electrode is designed to have a total length of 10.5 m (arch length is somewhat greater than 120 degrees) and its ends are slightly bent for the purpose of eliminating the flashovers caused by border effect. Also, when the rotor is turning an approximately uniform flashovers distribution has been detected along the arch (Table 1). Therefore, the choice of arching electrode is a very realistic arrangement for the experiments.

All tests were conducted according to current standard [8]. The experiments were performed for three typical rotational speeds of the wind turbine blades:

CASE I: $w = 0$ r/min, when the wind turbine is fixed with one blade vertical;
CASE II: $w = 250$ r/min, for the winds of moderate strength;
CASE III: $w = 400$ r/min, rated rotor speed.

Table 1. Number of flashovers along the arching electrode for negative switching impulse voltage

Rotational speed of the blades	Position along the arching electrode α [°]					
	[-60°, -40°]	[-40°, -20°]	[-20°, 0°]	[0°, 20°]	[20°, 40°]	[40°, 60°]
	Number of flashovers (F)					
$w = 0$ r/min one blade is straight up	0	0	4	5	1	0
$w = 0$ r/min one blade is straight down	3	2	0	0	1	4
$w = 250$ r/min	2	1	2	1	2	2
$w = 400$ r/min	2	1	1	1	2	3

The observed range of rotational speeds w for the reduced-size wind turbine model corresponds to the range of rotational speeds 0–25 r/min for the actual wind turbine, according to the formula: $v_t = \pi w l_b x\, 30^{-1}$, where v_t [m/s] is the peripheral blade tip speed, w [r/min] is the rotational speed of the blades, and l_b [m] is the blade length.

It is important that the number of discharges in laboratory conditions is comparable with the expected conditions for the actual wind turbine location. In each of the analyzed cases $n = 20$ discharges with negative polarity were implemented,

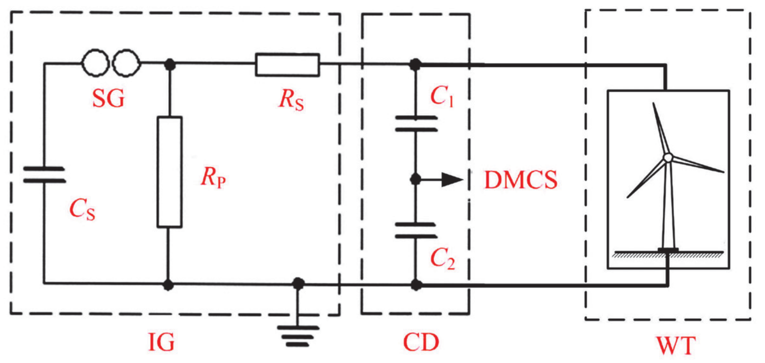

IG - Impulse generator; CD - Capacitive voltage divider; SG - Spark-gap; Rs - equivalent serial resistance of impulse generator; Rp - equivalent parallel resistance of impulse generator; Cs - equivalent capacity of impulse generator; WT - Reduced-size wind turbine model; DMCS - Digital measuring and control system.

Figure 4. Measuring and control system in the high-voltage laboratory

giving information on the areas of wind turbine blades that will possibly trigger a lightning strike by incepting leaders towards the arching high-voltage electrode.

A standard switching impulse voltage waveform 250/2500 μs was applied to the arching electrode with amplitude sufficient to create a flashover (Figs. 3–4). Switching impulse voltage is usually taken as the most representative for the electric field in the vicinity of a wind turbine during an initial leader attachment. Flashover should take place on the rising front of the impulse wave and close to the peak.

Up-and-down method was applied for determining 50% switching flashover voltage (FOV) in all the cases examined. When the FOV is normally distributed (according to Gaussian distribution) the up-and-down method permits a quite reliable estimation of the 50% FOV [9]. Before the beginning of each measuring set, the initial voltage U_{00} was chosen at which with certainty no flashover occurs. The voltage is then initially raised in steps of an approximately constant amplitude Δu until the first flashover occurs at a voltage U_{l1} (Fig. 6(A)-(C)). The voltage is then reduced by Δu. If no flashover occurs at voltage $U_{l2} = U_{l1} - \Delta u$, the test voltage should again be raised through Δu, otherwise be reduced by Δu.

The process is repeated until a predetermined number n of voltage values U_{l1}, U_{l2},… U_{ln}, are obtained. With a large sample n, the arithmetic mean of these voltages in itself provides a preliminary estimate of the required 50% FOV. If the number of strikes was defined as n_l at any level U_l, the 50% FOV can be calculated as follows:

$$U_{50<_{FOV}} = \frac{\sum_{l=1}^{n=20} n_l U_l}{\sum_{l=1}^{n=20} n_l} \tag{1}$$

The first voltage level previously being adopted was the one having two or more strikes, in order to avoid mistakes if the initial voltage was chosen too low or high. The 10% FOV was also determined on the basis of the Gaussian distribution. Uncertainty for determined voltage peak value was 1.6%. The stated uncertainty is expanded one, obtained by multiplying the standard uncertainty by a coverage factor $k = 2$. The value of a measuring results lies within the assigned range of values with a probability of 95%.

3. EXPERIMENTAL RESULTS

It is well known that more than 90% of natural lightning flashes are of negative polarity and the wind turbines are mostly exposed to upward initiated lightning. Also, the majority of actual wind turbines have the air-termination system in the form of lightning receptors on the tips of the blades. These cases are examined in detail.

A comprehensive analysis when a negative impulse voltage is applied to the arching electrode is presented in Figs. 5–7. Based on the Fig. 5 can be observed that the connection points of leaders from the arching electrode and the corresponding blade are located closer to the arching electrode. However, concurrently with the increase in the rotational speed of wind turbine blades the connection points are moved a little closer to the blade tip and the discharges from the arching electrode are extended deeper into the gap.

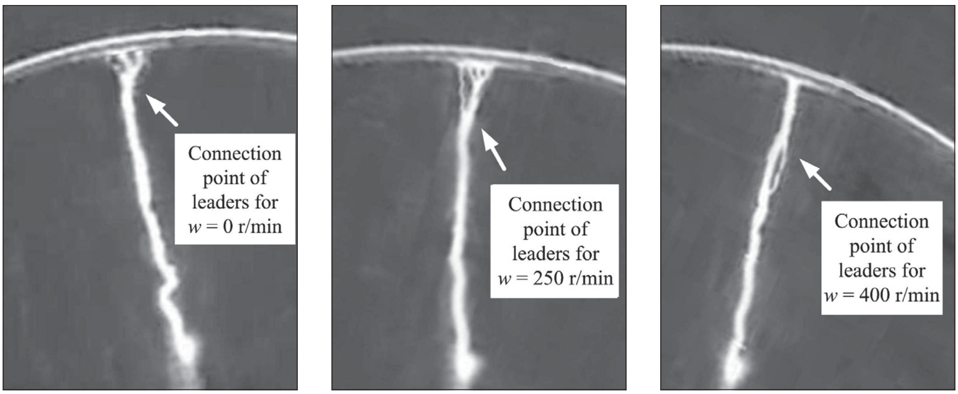

Figure 5. Enlarged photos of typical leaders connection

Table 2. Discharge manner, FOV, and relative increase and dispersions of FOV for the analyzed cases

Rotational speed w = 0 r/min		Rotational speed w = 250 r/min		Rotational speed w = 400 r/min	
Discharge manner	No. of times	Discharge manner	No. of times	Discharge manner	No. of times
Electrode-to-ground	0	Electrode-to-ground	1	Electrode-to-ground	2
Receptor	9	Receptor	8	Receptor	7
Penetration/damage	1	Penetration/damage	1	Penetration/damage	1
$U_{50\%\ 0\ \mathrm{r/min}}$	-1139.0 kV	$U_{50\%\ 250\ \mathrm{r/min}}$	-1171.5 kV	$U_{50\%\ 400\ \mathrm{r/min}}$	-1246.2 kV
$U_{10\%\ 0\ \mathrm{r/min}}$	-1047.9 kV	$U_{10\%\ 250\ \mathrm{r/min}}$	-1077.8 kV	$U_{10\%\ 400\ \mathrm{r/min}}$	-1146.5 kV
$U_{50\%\ 250\ \mathrm{r/min}}/U_{50\%\ 0\ \mathrm{r/min}}$	1.028 p.u.	$U_{50\%\ 400\ \mathrm{r/min}}/U_{50\%\ 0\ \mathrm{r/min}}$	1.094 p.u.	$U_{50\%\ 400\ \mathrm{r/min}}/U_{50\%\ 250\ \mathrm{r/min}}$	1.064 p.u.
$\sigma_{250\ \mathrm{r/min}}/\sigma_{0\ \mathrm{r/min}}$	1.081 p.u.	$\sigma_{400\ \mathrm{r/min}}/\sigma_{0\ \mathrm{r/min}}$	1.122 p.u.	$\sigma_{400\ \mathrm{r/min}}/\sigma_{250\ \mathrm{r/min}}$	1.087 p.u.

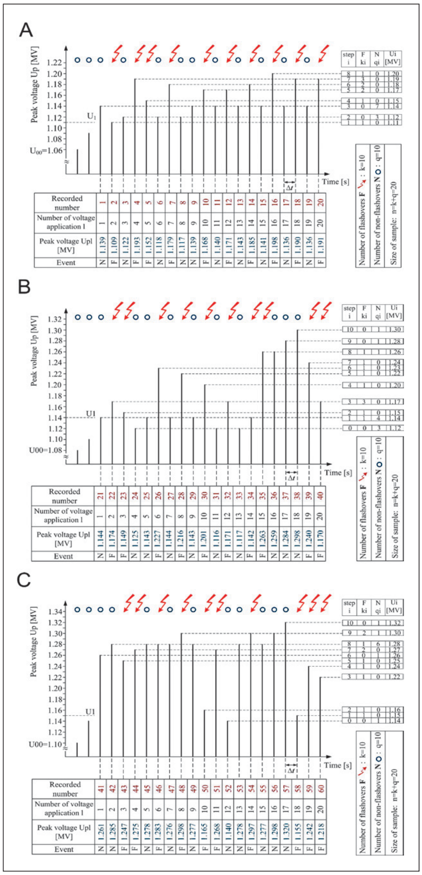

Figure 6. Up-and-down method when a negative impulse voltage is applied to the arching electrode. (A) w = 0 r/min; (B) w = 250 r/min; (C) w = 400 r/min

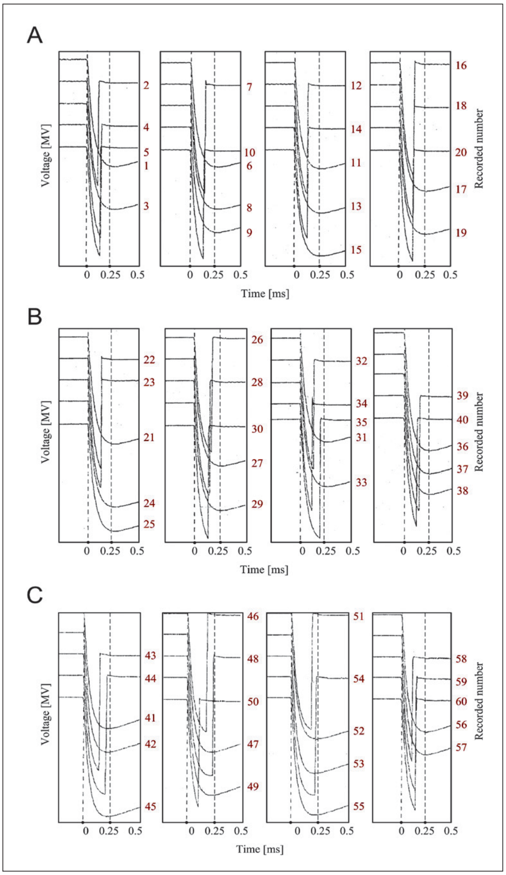

Figure 7. Characteristic waveforms when a negative impulse voltage is applied to the arching electrode. (A) w = 0 r/min; (B) w = 250 r/min; (C) w = 400 r/min

The FOV rise for w = 250 r/min in relation to the FOV for w = 0 r/min for 2.9% can be observed, as well as the FOV rise for w = 400 r/min in relation to the FOV for w = 0 r/min for 9.4% (Table 2). In all three cases, a slight increase in the number of electrode-to-ground lightning discharges was observed. This effect becomes more pronounced when the rotational speed increases.

By analyzing the enlarged voltage waveforms, it can be concluded that slight increase in wave oscillation occurs concurrently with the increase in the rotational speed of the wind turbine blades, particularly in the zone near the peak values of the flashover voltage (Fig. 7(A)-(C)). It was detected that increase in the dispersion σ of flashover voltages occurs simultaneously with the increase in the rotational speed (Table 2). Likewise, the mean value of the wave time to flashover was increased concurrently with the increase in the rotational speed.

4. DISCUSSION

The experimental results show the following; concurrently with the increase in rotational speed of wind turbine blades the number of direct lightning strikes to the blades, when the discharge struck receptor directly or penetrate/damaged the blade tip, slightly decreased (see Table 2). The influence of blade rotation becomes more dominant with the increase in rotational speed of the blades. Effect of blade rotation on the 50% switching FOV, which are obtained based on the up-and-down method, is shown in Fig. 8.

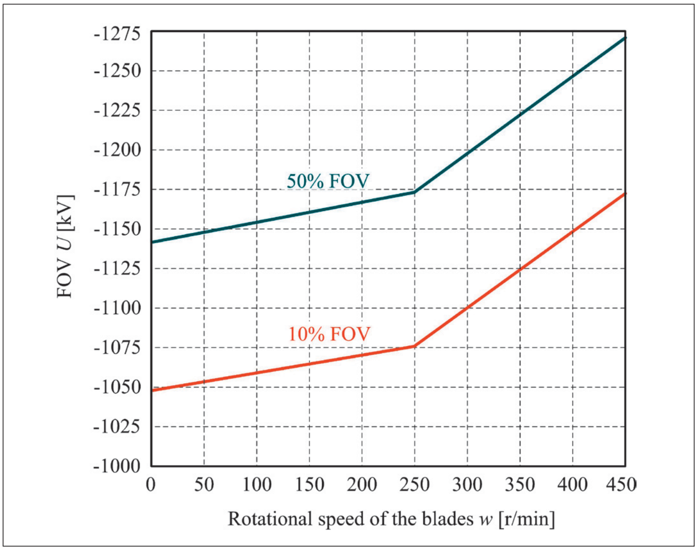

Figure 8. Impact of blade rotation on the 50% and 10% FOV

The consistent increase in FOV occurs due to a separation of space charge from the blade tip. At w = 250 r/min a blade tip moves 6.3 mm during the 200 μs time that an impulse voltage is increasing before flashover. In some cases of lightning discharge, the blade tip moves very little after the applied electric field has become sufficient to initiate corona at the blade. The increase in 50% FOV compared to the case when the wind turbine is idle is relatively small (about 3%).

But it must be noted that at w = 400 r/min (rated rotor speed) the blade tip moves about 1 cm during the 200 μs time and the increase in 50% FOV compared to the w = 0 r/min is noticable (about 10%). The initial leader may "sweep" along the blade surface a short distance prior to first stroke arrival. The original ionized channel may shift and can be extended as the rotating tip moves away from it. The cumulative effect of increased space charge dispersion in the zone of the air-termination system on the blades, caused by strong wind circulation near the blades, is more pronounced in this case.

The conclusion that blades of a moving rotor are less likely to get struck by lightning than are blades that are stationary can be gained based on the typical photos of the test flashovers, especially of their positions along the arch (see Table 1), and of the connection locations in typical flashover between approaching and junction leaders (see Fig. 5). It is important to note that each test procedure was recorded using two digital cameras, but a certain number of photos of the test flashovers could not be obtained with a satisfactory quality, because the blades were mostly rotated at very high speeds. A tendency that concurrently with the increase in rotational speed of the blades the connection points of leaders from the arching electrode and the corresponding blade are moved a little closer to the blade tip, can be observed.

On the basis of everything stated above, it can be concluded that the overall effects of the analyzed phenomena at speeds w = 250 r/min and 400 r/min are congruent. The obtained results substantiate the conclusion about lightning susceptibility of rotating versus stationary rotor blades in laboratory conditions.

5. CONCLUSION

The following main results were obtained.

1) When the rotor of the reduced-size wind turbine is turning, a slight decrease in the number of direct lightning strikes in the zone of the air-termination system on the blades was observed, in regard to the case when the rotor is stationary. Also, when the blades are rotating an increase of 50% FOV was recorded according to the up-and-down method and the connection points of leaders from the arching electrode and the corresponding blade are moved a little closer to the blade tip. These effects become more dominant as the rotational speed of the blades increases.

2) In the cases when the blades are rotating, increasing dispersion of FOV and somewhat more pronounced transience of voltage waveforms, were noticed.

3) During the high-voltage testing with a rotating model a certain number of unexpected results was obtained. According to the theory of similarity the derived general conclusions can be extrapolated to actual wind turbines. It is quite realistic to assume that there is a difference in the lightning attachment process whether the real blades are rotating or not. However, it is necessary to verify and validate the obtained results in service. It is also important to conduct further research.

6. FUTURE WORK

The opportunity to test a rotating wind turbine is very attractive. Instead of the arching electrode can be used a single rod electrode (to represent a downward leader at an assumed striking distance) at discrete positions along the arch described by the present arching electrode. As an alternative and a third solution the authors will consider the possibility to use several rod electrodes at discrete positions along the arch (three rod electrodes along the left and right segment of the arch). The authors will also consider testing in a wind tunnel when the blade is steady and the air is moving by using a real blade tip and similar velocities as in the real world.

LITERATURE

[1] M. S. Savić and Z. Stojković, *High-Voltage Techics, Lightning Impulses*, Faculty of Electrical Engineering, Belgrade, 506 p, 1997.

[2] B. Radičević, D. Mikičić and Ž. Đurišić, *Estimation of Wind Power*, Facta Universitatis, Series: Electronics and Energetics, vol. 19, no. 1, pp. 47–61, 2006.

[3] T. Naka, N. J. Vasa, S. Yokoyama, A. Wada, A. Asakawa, H. Honda, K. Tsutsumi and S. Arinaga, *Study on lightning protection methods for wind turbine blades*, IEEJ Trans. PE, Vol. 125, No. 10, 2005.

[4] I. Cotton, N. Jenkins and K. Pandiaraj, *Lightning Protection For Wind Turbine Blades And Bearings,* Wind Energy Journal, vol. 4, no. 1, pp. 23–37, March 2001.

[5] S. F. Madsen, J. Holboll, M. Henriksen, K. Bertelsen and H.V. Erichsen, *New test method for evaluating the lightning protection system on wind turbine blades*, Proc. of the 28th International Conference on Lightning Protection, Kanazawa, Japan, pp. 1497–1502, 18–22 September 2006.

[6] S. F. Madsen and H.V. Erichsen, *Numerical model to determine lightning attachment point distributions on wind turbines according to the revised IEC 61400–24*, Proc. of the International Conference on Lightning and Static Electricity *(*ICOLSE*)*, Pittsfield, Massachusetts, USA, 15–17 September 2009.

[7] O. Anaya-Lara, N. Jenkins, J. Ekanayake, P. Cartwright, and M. Hughes, *Wind Energy Generation: Modelling and Control.* Glasgow, U.K.: Wiley–Blackwell, 2009, p. 288.
[8] IEC 61400–24, International Standard, Ed. 1.0, *Wind turbines – Part 24: Lightning protection*, International Electrotechnical Commission, Geneva, Switzerland, June 2010.
[9] W. Hauschild and W. Mosch, Statistical Techniques for High-Voltage Engineering. London, U.K.: P. Peregrinus Ltd., 1992, p. 324.

UTICAJ ROTACIJE ELISA VJETROTURBINE NA UČESTALOST ATMOSFERSKOG PRAŽNJENJA

Sažetak: Uticaj rotacije elisa vjetroturbine na karakteristike atmosferskog pražnjenja nije dovoljno proučen. Eksperimentalni rezultati, koji su prikazani u ovom radu, treba da omoguće bolje razumijevanje ovog fenomena. Ispitivanje je obavljeno u visokonaponskoj laboratoriji, primjenjujući metodu gore-dolje za određivanje 50% preskočnog sklopnog standardnog udarnog napona. Impulsni naponski talasi su primijenjeni između specijalno konstruisane lučne elektrode i elisa modela vjetroturbine umanjenih dimenzija, koji je vjeran originalu, pokretanog pomoću frekventno upravljanog indukcionog motora. Ispitivanje je izvršeno za gromobranski zaštitni sistem u vidu receptora tipa dugme na vrhovima elisa vjetroturbine. Na osnovu teorije sličnosti u radu su analizirane osobine direktnog atmosferskog pražnjenja u zoni prihvatnog sistema na elisama vjetroturbine, za nekoliko karakterističnih brzina obrtanja. Glavni zaključak je da se broj direktnih udara u vrhove elisa smanjuje zbog rotacije vjetroturbine u odnosu na slučaj kada su elise nepomične.

Ključne riječi: *prihvatni sistem, lučna elektroda, elipse, preskočni napon (PON), indukcioni motor, gromobranska zaštita, umanjen model, rotacija, metoda gore-dolje, vjetroturbina*